

# Image Segmentation using Distance Regularized Level Set Method

Mr. Gaikwad Avinash S., Dr. Bhalerao Deepashree M.

**Abstract**— Level set methods have been mostly used in image Processing and computer vision applications. In conventional level set function generally generates the irregularities during its evolution, which may increase numerical errors and lose the stability of the evolution. Hence degraded Level set function periodically replace by numerical remedy called reinitialization with a signed distance function. However, the reinitialization raises serious problems as when and how it should be performed, but also affects numerical accuracy. To avoid this, in proposed method level set evolution is designed as the gradient flow that minimizes energy function with a distance regularization term and an external energy that drives the motion of the zero level set toward desired locations. The distance regularization term is defined with a potential function such as Single Well, Double Well, Triple Well, Quad Well & Huber such that the derived level set evolution has forward-and-backward (FAB) diffusion effect, which is able to maintain a desired shape of the level set function, particularly a signed distance profile near the zero level set. This proposes a new type of level set evolution called distance regularized level set evolution (DRLSE). The distance regularization of level set function eliminates the need for reinitialization and reduced the induced numerical errors. DRLSE uses the more general and efficient initialization of the level set function which able to use relatively large time steps in the finite difference scheme to reduce the number of iterations, while ensuring sufficient numerical accuracy. To demonstrate the effectiveness of the DRLSE formulation, we apply it to an edge-based active contour model for image segmentation

**Index Terms**—Distance regularized level set function, Potential function, Reinitialization.

## I. INTRODUCTION

The Level set method was introduced by Osher & Sethian [2] in 1987 to capture dynamic interfaces and shapes. The basic idea of the level set method is to represent a contour as the zero level set of a higher dimensional function, called a level set function (LSF), and formulate the motion of the contour as the evolution of the level set function. Level set method able to represent contours of complex topology and are able to handle topological changes, such as splitting and merging, in a natural and efficient way, which is not allowed in parametric active contour models [7], [9], [10] unless extra indirect procedures are introduced in the implementations. Also another desirable feature of level set methods is that numerical computations can be performed on a fixed Cartesian grid without having to parameterize the points on a contour as in parametric active contour models. Level set methods are used to solve a wide range of scientific and engineering problems, their applications have been suffer with the irregularities of the Level set function. In conventional level set methods, the LSF develops

irregularities during its evolution, which generates the numerical errors and loses the stability of the level set evolution. This problem is avoided by numerical remedy, called as reinitialization [20], [21], Reinitialization is achieved by periodically stopping the evolution and reshaping the degraded LSF as a signed distance function [22], [21]. The proposed variation level set formulation with a distance regularization term with an external energy term that drive the motion of the zero level contour toward desired locations. The distance regularization term is defined with a potential function such that it forces the gradient magnitude of the level set function to one of its minimum points, for maintaining the desired shape of the level set function, particularly a signed distance profile near its zero level set. As Potential function, single well, double well, triple Well, quad Well & huber function is used. Where well indicates the minimum point & number indicates the number of repetitions. In proposed method, we provide a double-well, triple well, quad well & Huber potential for the distance regularization term. The level set evolution is derived by gradient flow that minimizes the energy functional. Regularity of the LSF is maintained by a forward-and-backward (FAB) diffusion derived from the distance regularization term. As a result, the distance regularization eliminates the need for reinitialization. To demonstrate the effectiveness of the DRLSE formulation, we apply it to an edge-based active contour model. Due to the distance regularization term, the DRLSE can be implemented with a simpler and more efficient numerical scheme in both full domain and narrowband implementations than conventional level set formulations. Moreover, relatively large time steps can be used to significantly reduce the number of iterations and computation time, while ensuring sufficient numerical accuracy.

## II. PROPOSED DISTANCE REGULARIZED LEVEL SET FUNCTION (DRLSE)

In DRLSE, Level set function designed as the gradient flow that minimizes energy function with a distance regularization term and an external energy that drives the motion of the zero level set toward desired locations. The distance regularization term is defined with a potential function such as Single Well, Double Well, Triple Well, Quad Well & Huber such that the derived level set evolution has forward-and-backward (FAB) diffusion effect, which is able to maintain a desired shape of the level set function, particularly a signed distance profile near the zero level set. Let  $\phi: \Omega \rightarrow \mathcal{R}$  be a LSF defined on a domain  $\Omega$ . Energy function  $\epsilon(\phi)$  defined as as

$$\epsilon(\phi) = \mu \mathcal{R}_p(\phi) + \epsilon_{\text{ext}}(\phi) \quad (1)$$

Where  $\varepsilon(\phi)$  is energy Function,  $\mathcal{R}_p(\phi)$  is level set regularization term defined as follows &  $\varepsilon_{\text{ext}}(\phi)$  is external energy that depends upon the data of interest &  $\mu$  is constant whose value is greater than zero.

The initial Level set function  $\phi$  defined on a domain  $\Omega$  as shown below,

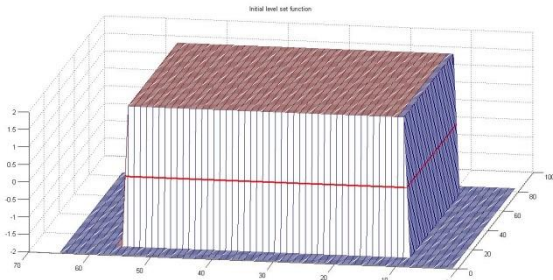


Fig. 1 Initial Level Set Function  $\phi$  for Two Cell Image.

The level set regularization term  $\mathcal{R}_p(\phi)$  is defined by following equation,

$$\mathcal{R}_p(\phi) = \int_{\Omega} p(|\nabla\phi|) dX \quad (2)$$

Where  $p$  is a potential function. The external energy  $\varepsilon_{\text{ext}}(\phi)$  is designed to achieve a minimum when the zero level set of the LSF is located at desired position.

#### A. Gradient Flow for Energy Minimization

Energy functional  $F(\phi)$  is minimize by finding the steady state solution of the gradient flow equation as follows,

$$\frac{\partial\phi}{\partial t} = -\frac{\partial F}{\partial\phi} \quad (3)$$

Where  $\frac{\partial F}{\partial\phi}$  is the Gâteaux derivative of the Energy functional  $F(\phi)$ . Gâteaux derivative of the functional  $\mathcal{R}_p(\phi)$  is obtained as follows.

$$\frac{\partial\mathcal{R}_p}{\partial\phi} = -\mu \operatorname{div}(d_p(|\nabla\phi|\nabla\phi)) \quad (4)$$

Where  $\operatorname{div}(\cdot)$  is divergence operator and  $d_p$  is obtained by,

$$d_p = \frac{p'(s)}{s} \quad (5)$$

Where  $p'(s)$  is the first derivative of potential functional. Where potential function may double well, triple well, quad well or huber Function. From equation no (1),

$$\frac{\partial\varepsilon}{\partial\phi} = \mu \frac{\partial\mathcal{R}_p}{\partial\phi} + \frac{\partial\varepsilon_{\text{ext}}}{\partial\phi} \quad (6)$$

Where  $\frac{\partial\varepsilon_{\text{ext}}}{\partial\phi}$  is Gâteaux derivative of the external energy functional  $\varepsilon_{\text{ext}}$  with respect to  $\phi$ .

$$\frac{\partial\phi}{\partial t} = \mu \operatorname{div}(d_p(|\nabla\phi|\nabla\phi)) - \frac{\partial\varepsilon_{\text{ext}}}{\partial\phi} \quad (7)$$

Above PDE is called as DRLSE which preserve the signed distance property of the LSF, which is associated with the Distance regularization term  $\mathcal{R}_p(\phi)$ . The gradient flow of Energy  $\mu\mathcal{R}_p(\phi)$  shows the effect of distance regularization in DRLSE.

$$\frac{\partial\phi}{\partial t} = \mu \operatorname{div}(d_p(|\nabla\phi|\nabla\phi)) \quad (8)$$

$$\frac{\partial\phi}{\partial t} = \operatorname{div}(D\nabla\phi) \quad (9)$$

Where diffusion rate  $D = -\mu \operatorname{div}(d_p(|\nabla\phi|))$ . Diffusion rate can be positive or negative. If the diffusion rate is positive, the diffusion is Forward, which decreases the  $|\nabla\phi|$ . While if diffusion rate is negative, the diffusion is Backward which increases the  $|\nabla\phi|$ . This diffusion is called as Forward and backward Diffusion (FAB) [1]. This FAB diffusion adaptively increases or decreases to force it to be close to one of the minimum points of the potential function  $p(s)$ , thereby maintaining the desired shape of the function  $\phi$ .

#### B. Potential Function

In proposed method contains the different potential function such as Single well, Double well, Triple Well, Quad Well & Huber. Where well indicates the function minimum point while number indicates the number of wells. Huber function contain the single minima at  $s=1$ .

A good potential function for the regularization term has ability to force the level set function to be zero. Such a level set regularization term has a strong smoothing effect, but may flatten the LSF and finally make the zero level contour disappear. Purpose of introducing the level set regularization term is not only to smooth the LSF, but also to maintain the signed distance property, at least in a vicinity of the zero level set, in order to ensure accurate computation for curve evolution.

Single well Potential Function as minimum points at  $s=1$ . Hence distance regularization term with Single well potential function is defined as follows,

$$p = p_1(s) = \frac{1}{2}(s-1)^2 \quad (10)$$

With single well potential function  $p = p_1(s)$ , level set regularization term  $\mathcal{R}_p(\phi)$  is defined as,

$$P(\phi) = \frac{1}{2} \int_{\Omega} (|\nabla\phi| - 1)^2 dX \quad (11)$$

However, the derived level set evolution with Single well potential function for energy minimization has an undesirable side effect on the LSF in some circumstances. This problem is avoided by taking the minimum points at  $s=0$  &  $s=1$ , which is called as Double well Potential Function. Such a potential is a double-well potential  $p_2(s)$  as it has two minimum points (wells).

$$p = p_2(s) = \begin{cases} \frac{1}{(2\pi)^2} (1 - \cos(2\pi s)) & \text{if } s \leq 1 \\ \frac{1}{2}(s-1)^2 & \text{if } s > 1 \end{cases} \quad (12)$$

Triple well Potential Function  $p_3(s)$  is defined as follows. Which has minima at three different points  $s=0$ ,  $s=0.5$  &  $s=1$ .

$$p = p_3(s) = \begin{cases} \frac{1}{(2\pi)^2} (1 - \cos(4\pi s)) & \text{if } s \leq 1 \\ \frac{1}{2}(s-1)^2 & \text{if } s > 1 \end{cases} \quad (13)$$

Quad well Potential Function  $p_4(s)$  is defined as follows. Which has minima at four different points  $s=0$ ,  $s=0.33$ ,  $s=0.66$  &  $s=1$ .

$$p = p_4(s) = \begin{cases} \frac{1}{(2\pi)^2} (1 - \cos(6\pi s)) & \text{if } s \leq 1 \\ \frac{1}{2}(s-1)^2 & \text{if } s > 1 \end{cases} \quad (14)$$

Huber potential function has single minima at  $s=1$  while on both side of minima magnitude of potential function is increases in logarithmic scale as expressed below,

$$\rho_1 = \frac{\Delta_0^2}{2} \left( \sqrt{1 + \frac{4\phi_1(s)}{\Delta_0^2}} \right) \quad (15)$$

Where  $\Delta_0$  is constant value,  $\phi_1(s) = e^2$  where  $e = s_k - s_r$ . Following fig. 1 shows various potential functions,

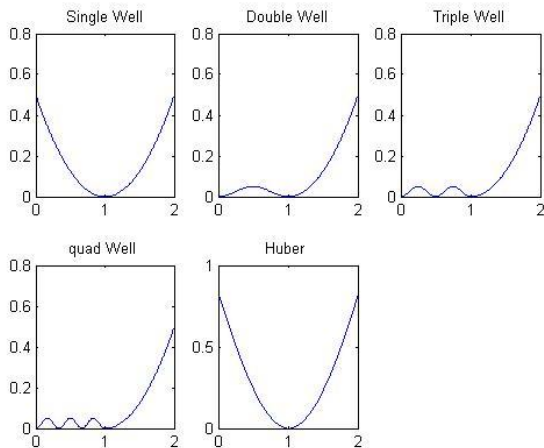


Fig. 2 a) Single Well Potential Function b) Double Well Potential Function c) Triple Well Potential Function d) Quad Well Potential Function e) Huber Well Potential Function.

### C. External Energy $\varepsilon_{ext}(\phi)$

Let be  $I$  an image on a domain  $\Omega$  & edge indicator function  $g$  is defined as

$$g = \frac{1}{1 + |\nabla G_\sigma * I|^2} \quad (16)$$

Where  $G_\sigma$  is a Gaussian kernel with a standard deviation. Gaussian kernel is used to smooth the image to reduce the noise. Edge indicator function takes smaller values at object boundaries than at other locations.

For an LSF, we define an external energy functional  $\varepsilon_{ext}(\phi)$  by following equation,

$$\varepsilon_{ext}(\phi) = \lambda L_g(\phi) + \alpha A_g(\phi) \quad (17)$$

Where  $\lambda$  &  $\alpha$  are constants whose values is greater than zero,  $L_g(\phi)$  is Line integral of function of  $g$  along the zero level contour of  $\phi$ ,  $A_g(\phi)$  is weighted area of region  $\phi$ .  $L_g(\phi)$  is Line integral of function is minimized when the zero level contour  $\phi$  is located at the object boundaries. Where  $A_g(\phi)$  weighted area is introduced to speed up the motion of the zero level contour in the level set evolution process, which is necessary when the initial contour is placed far away from the desired object boundaries. Mathematically  $A_g(\phi)$  &  $L_g(\phi)$  is expressed as follows.

$$L_g(\phi) = \int_{\Omega} g \delta(\phi) |\nabla \phi| dx \quad (18)$$

$$A_g(\phi) = \int_{\Omega} g H(-\phi) dx \quad (19)$$

Where  $\delta$  &  $H$  are the dirac delta function & Heaviside Function respectively. In practice, the Dirac delta function  $\delta$  and Heaviside function  $H$  in the functional  $L_g$  and  $A_g$  are approximated by the following smooth functions  $\delta_\varepsilon$  and  $H_\varepsilon$  as in many level set methods [20], defined by

$$\delta_\varepsilon(x) = \begin{cases} \frac{1}{(2\varepsilon)} \left(1 + \cos\left(\frac{\pi x}{\varepsilon}\right)\right) & \text{if } |x| \leq \varepsilon \\ 0 & \text{if } |x| > \varepsilon \end{cases} \quad (20)$$

$$H_\varepsilon(x) = \begin{cases} \frac{1}{(2)} \left(1 + \frac{x}{\varepsilon} + \frac{1}{\pi} \sin\left(\frac{\pi x}{\varepsilon}\right)\right) & \text{if } |x| \leq \varepsilon \\ 1 & \text{if } |x| > \varepsilon \\ 0 & \text{if } |x| < -\varepsilon \end{cases} \quad (21)$$

With dirac delta function  $\delta$  & Heaviside function  $H$  in (18) & (19) replaced by  $\delta_\varepsilon$  &  $H_\varepsilon$ , the energy functional  $\varepsilon(\phi)$  is then approximated by,

$$\varepsilon(\phi) = \mu \int_{\Omega} p(|\nabla \phi|) dX + \lambda \int_{\Omega} g \delta_\varepsilon(\phi) |\nabla \phi| dx + \alpha \int_{\Omega} g H_\varepsilon(-\phi) dx \quad (22)$$

above energy functional is minimized by solving the following gradient flow,

$$\frac{\partial \phi}{\partial t} = \mu \operatorname{div}(d_p(|\nabla \phi|) \nabla \phi) + \lambda g \delta_\varepsilon(\phi) \operatorname{div}\left(g \frac{\nabla \phi}{|\nabla \phi|}\right) + \alpha g H_\varepsilon(-\phi) \quad (23)$$

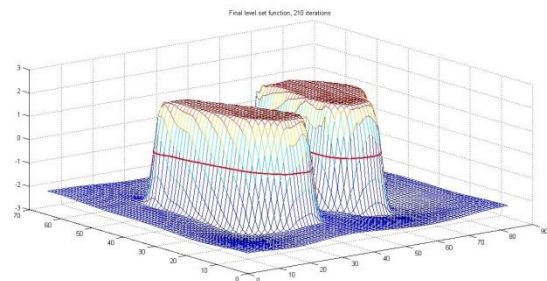


Fig. 3 The final level set function  $\phi$  by minimizing the gradient flow equation for Two Cell Image.

The first term on the right hand side in equation no (23) is associated with the distance regularization energy  $\mathcal{R}_p(\phi)$ , while the second and third terms are associated with the energy terms  $L_g(\phi)$  and  $A_g(\phi)$ , respectively. Equation (23) is an edge-based geometric active contour model.

## III. ALGORITHM & FLOW CHART OF IMPLEMENTATION

### A. Algorithm

- Step 1: Input image smoothing by using Gaussian kernel (16).
- Step 2: Define initial level set function  $\phi_0$ .
- Step 3: Obtain partial differentiation of Edge Indicator Function  $g$  (27) of original Image.
- Step 4: Compute Distance Regularization Term (2).
- Step 5: Compute Dirac delta function  $\delta_\varepsilon$  (20) & Heaviside function  $H_\varepsilon$  (21).
- Step 6: Compute Energy Functional (23).
- Step 7: If either the zero crossing points stop varying for consecutive iterations or exceeds a prescribed maximum number of iterations, then stop the iteration, otherwise, go to Step 3.

### B. Flow Chart

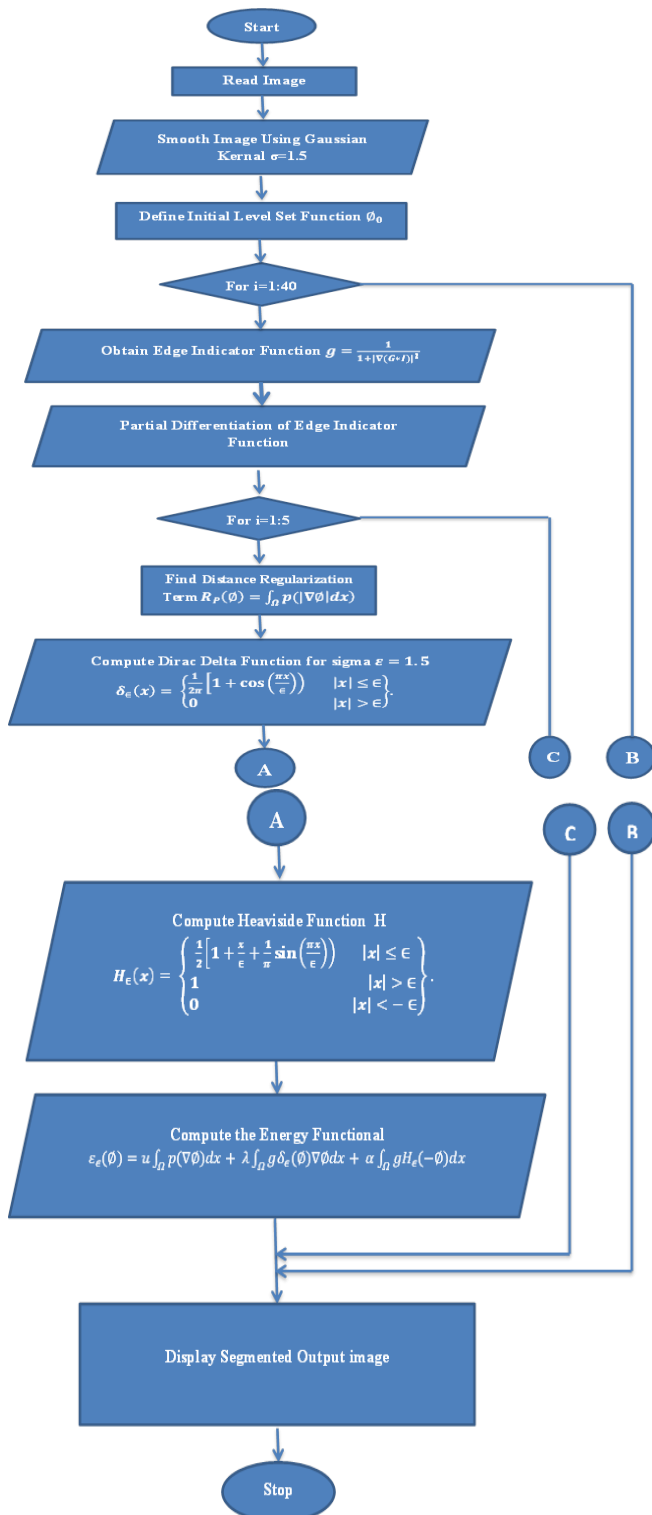


Fig. 4 Algorithm of DRLSE Implementation

IV. RESULTS

The performance of DRLSE obtained by considering the various parameters such as effect of constant terms on the evolution of LSF, by comparing the True coordinator of Synthetic Image with obtained coordinator for various potential functions which is also called as Mean square Error MSE i.e. Euclidian distance between coordinator of True Image Contour & Obtained contour for various Potential functions, CPU computation time of DRLSE for various Potential functions.

The DRLSE results obtained for both Synthetic & Real Images. The proposed DRLSE algorithm contains the

constant like  $\alpha, \mu, \lambda$  and time step  $\Delta t$ . Performance of proposed algorithm is not affected by  $\mu$  &  $\lambda$ . For obtaining the result typical values of constants are as  $\lambda = 5, \mu = 0.04$  &  $\Delta t = 5$ . All the constant parameters need to be tuned according to the image. A nonzero  $\alpha$  provides additional external force to drive the motion of the contour, which may deviate final contour from the true object boundary due to the shrinking or expanding effect of the weighted area term. This deviation can be refining by further evolving the contour for a few iterations with the parameter  $\alpha = 0$ . For images with weak object boundaries, a large value of may cause boundary leakage, i.e., the active contour may easily pass through the object boundary. Therefore, for images with weak object boundaries the value of  $\alpha$  should be chosen relatively small. Following images shows Final Segmented Image using DRLSE. For computation of DRLSE the parameters are selected as, time step  $\Delta t = 5, \mu = \frac{0.2}{\Delta t}$ , Gaussian Kernel scale  $\sigma = 1.5$ , Width of the Dirac Delta function  $\epsilon = 1.5$ , coefficient of the weighted length term  $L(\phi) \lambda = 5$ , coefficient of the weighted area term  $A(\phi) \alpha = 1.5$ .

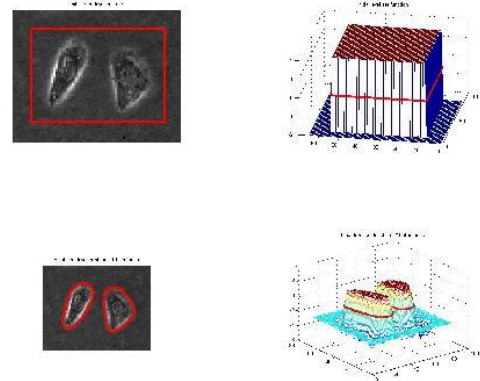


Fig. 5 a) Initial Zero Level Contour b) Initial Level set function c) Final Zero Level Contour d) Final Level set function for Original Two Cell Image.

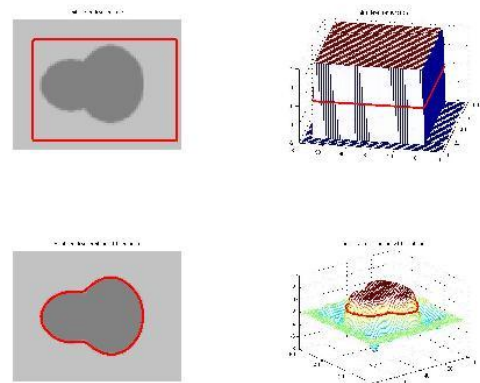


Fig. 6 a) Initial Zero Level Contour b) Initial Level set function c) Final Zero Level Contour d) Final Level set function for Original Gourd Image.

The true object boundaries are known for the synthetic images, which can be used to evaluate the accuracy of the

segmentation results. A metric to evaluate the accuracy of a segmentation result is the mean error defined by,

$$e(C) = \frac{1}{N} \sum_{n=1}^N \text{dist}(P_i, S) \quad (24)$$

Where S is True object Contour Coordinates,  $P_1, P_2, \dots, P_N$  be the obtained coordinator points on contour C using various Potential Functions &  $\text{dist}(P_i, S)$  is the Euclidian distance between True object Contour coordinates & obtained coordinator points on contour C using various Potential Function. Following table 1. Shows the Euclidian distance for Two cell Image & Gourd Image using various Potential Function. Final contour obtained using Triple well & Quad well potential function achieves the maximum similarity i.e. less MSE 0.8826 for Gourd Image & 2.1097 for Two Cell Image respectively, as compared to other potential function.

Potential Function	Two Cell Image	Gourd Image
Single Well	2.1663	0.9043
Double Well	2.1316	0.9005
Triple Well	2.1253	0.8826
Quad Well	2.1097	0.9709
Huber	2.5199	1.4043

Table 1. Mean square errors for various Potential Function for Two cell & Gourd Image respectively

CPU times consumed for the three different images are recorded. DRLSE is implemented on Matlab 2014 version. The CPU times were obtained by running the program on a Dell XPS Laptop with Intel (R) Core (TM) i5 CPU, 4GB RAM. With same parameter for all three images i.e. time step  $\Delta t = 5$ ,  $\mu = \frac{0.2}{\Delta t}$ , Gaussian Kernel scale  $\sigma = 1.5$ , Width of the Dirac Delta function  $\varepsilon = 1.5$ , coefficient of the weighted length term  $L(\phi) \lambda = 5$ , coefficient of the weighted area term  $A(\phi) \alpha = 1.5$ . The CPU consumed time for contour obtained using Triple well & Quad well Potential Function is less as compared to other contour using Double well, Single well & Huber Potential Function.

Potential Function	Two Cell Image	Gourd Image	Character Image
Single Well	6.014381	6.213023	9.132854
Double Well	5.778856	6.206560	8.941343
Triple Well	6.505027	6.000688	13.092965
Quad Well	5.769963	6.311557	11.208121
Huber	6.528460	6.292171	12.025842

Table 2. CPU consumed time using different potential function for Two cell Image, Gourd Image & Character Image respectively (All times are in second).

## V. CONCLUSION

The proposed DRLSE with various Potential Functions has capability to maintain the regularity of Level set function, particularly the desirable signed distance property in a vicinity of the zero level set, which ensures accurate computation and stable level set evolution. DRLSE is implemented by a simpler and more computational efficient numerical scheme than conventional level set

methods. DRLSE is more flexible and provides efficient initialization for generating a signed distance function as the initial LSF. By varying the time step, proposed method able to reduce the iteration numbers and computation time, while maintaining sufficient numerical accuracy, due to the intrinsic distance regularization embedded in the level set evolution. The distance regularization of level set function eliminates the need for reinitialization and reduced the induced numerical errors. To demonstrate the effectiveness of the DRLSE formulation, proposed method applied to the edge-based active contour model for image segmentation.

## REFERENCES

- [1] Chunming Li, Chenyang Xu, Changfeng Gui, and Martin D. Fox, "Distance Regularized Level Set Evolution and Its Application to Image Segmentation" IEEE TRANSACTIONS ON IMAGE PROCESSING, VOL. 19, NO. 12, DECEMBER 2010
- [2] S. Osher and J. Sethian, "Fronts propagating with curvature-dependent speed: Algorithms based on Hamilton-Jacobi formulations," *J. Comput Phys.*, vol. 79, no. 1, pp. 12–49, Nov. 1988.
- [3] A. Dervieux and F. Thomasset, "A finite element method for the simulation of Rayleigh-Taylor instability," *Lecture Notes Math.*, vol. 771, pp. 145–158, 1980.
- [4] A. Dervieux and F. Thomasset, "Multifluid incompressible flows by a finite element method," *Lecture Notes Phys.*, vol. 141, pp. 158–163, 1980.
- [5] V. Caselles, F. Catte, T. Coll, and F. Dibos, "A geometric model for active contours in image processing," *Numer. Math.*, vol. 66, no. 1, pp. 1–31, Dec. 1993.
- [6] R. Malladi, J. A. Sethian, and B. C. Vemuri, "Shape modeling with front propagation: A level set approach," *IEEE Trans. Pattern. Anal. Mach. Intell.*, vol. 17, no. 2, pp. 158–175, Feb. 1995.
- [7] M. Kass, A. Witkin, and D. Terzopoulos, "Snakes: Active contour models," *Int. J. Comput. Vis.*, vol. 1, no. 4, pp. 321–331, Jan. 1987.
- [8] C. Xu, A. Yezzi, and J. Prince, "On the relationship between parametric and geometric active contours," in *Proc. 34th Asilomar Conf. Signals, Syst., Comput.*, Pacific Grove, CA, Oct. 2000, pp. 483–489.
- [9] S.-C. Zhu and A. Yuille, "Region competition: Unifying snakes, region growing, and Bayes/MDL for multiband image segmentation," *IEEE Trans. Pattern. Anal. Mach. Intell.*, vol. 18, no. 9, pp. 884–900, Sep. 1996.
- [10] C. Xu and J. Prince, "Snakes, shapes, and gradient vector flow," *IEEE Trans. Imag. Process.*, vol. 7, no. 3, pp. 359–369, Mar. 1998.
- [11] S. Kichenassamy, A. Kumar, P. Olver, A. Tannenbaum, and A. Yezzi, "Gradient flows and geometric active contour models," in *Proc. 5th Int. Conf. Comput. Vis.*, 1995, pp. 810–815.
- [12] V. Caselles, R. Kimmel, and G. Sapiro, "Geodesic active contours," *Int. J. Comput. Vis.*, vol. 22, no. 1, pp. 61–79, Feb. 1997.
- [13] R. Kimmel, A. Amir, and A. Bruckstein, "Finding shortest paths on surfaces using level set propagation," *IEEE Trans. Pattern Anal. Mach. Intell.*, vol. 17, no. 6, pp. 635–640, Jun. 1995.
- [14] C. Samson, L. Blanc-Feraud, G. Aubert, and J. Zerubia, "A variational model for image classification and restoration," *IEEE Trans. Pattern Anal. Mach. Intell.*, vol. 22, no. 5, pp. 460–472, May 2000.
- [15] N. Paragios and R. Deriche, "Geodesic active contours and level sets for detection and tracking of moving objects," *IEEE Trans. Pattern Anal. Mach. Intell.*, vol. 22, no. 3, pp. 266–280, Mar. 2000.
- [16] T. Chan and L. Vese, "Active contours without edges," *IEEE Trans. Image Process.*, vol. 10, no. 2, pp. 266–277, Feb. 2001. 3254 IEEE TRANSACTIONS ON IMAGE PROCESSING, VOL. 19, NO. 12, DECEMBER 2010
- [17] C. Li, C. Kao, J. C. Gore, and Z. Ding, "Minimization of region-scalable fitting energy for image segmentation," *IEEE Trans. Image Process.*, vol. 17, no. 10, pp. 1940–1949, Oct. 2008.
- [18] D. Cremers, "A multiphase levelset framework for variational motion segmentation," *Scale Space Meth. Comput. Vis.*, pp. 599–614, June 2003.
- [19] H. Jin, S. Soatto, and A. Yezzi, "Multi-view stereo reconstruction of dense shape and complex appearance," *Int. J. Comput. Vis.*, vol. 63, no. 3, pp. 175–189, July 2005.
- [20] J. Sethian, *Level Set Methods and Fast Marching Methods*. Cambridge, U.K.: Cambridge Univ. Press, 1999.
- [21] S. Osher and R. Fedkiw, *Level Set Methods and Dynamic Implicit Surfaces*. New York: Springer-Verlag, 2002.

- [22] M. Sussman, P. Smereka, and S. Osher, "A level set approach for computing solutions to incompressible two-phase flow," *J. Comput. Phys.*, vol. 114, no. 1, pp. 146–159, Sep. 1994.
- [23] M. Sussman and E. Fatemi, "An efficient, interface-preserving level set redistancing algorithm and its application to interfacial incompressible fluid flow," *SIAM J. Sci. Comput.*, vol. 20, no. 4, pp. 1165–1191, Jul. 1999.
- [24] D. Peng, B. Merriman, S. Osher, H. Zhao, and M. Kang, "A PDEbased fast local level set method," *J. Comput. Phys.*, vol. 155, no. 2, pp. 410–438, Nov. 1999.
- [25] G. Barles, H. M. Soner, and P. E. Souganidis, "Front propagation and phase field theory," *SIAM J. Control Optim.*, vol. 31, no. 2, pp. 439–469, Mar. 1993.
- [26] J. Gomes and O. Faugeras, "Reconciling distance functions and level sets," *J. Vis. Commun. Image Represent.*, vol. 11, no. 2, pp. 209–223, Jun. 2000.
- [27] M. Weber, A. Blake, and R. Cipolla, "Sparse finite elements for geodesic contours with level-sets," in *Proc. Eur. Conf. Comput. Vis.*, 2004, pp. 391–404.
- [28] C. Li, C. Xu, C. Gui, and M. D. Fox, "Level set evolution without re-initialization: A new variational formulation," in *Proc. IEEE Conf. Comput. Vis. Pattern Recognit.*, 2005, vol. 1, pp. 430–436.
- [29] G. Aubert and P. Kornprobst, *Mathematical Problems in Image Processing: Partial Differential Equations and the Calculus of Variations*. New York: Springer-Verlag, 2002.
- [30] L. Evans, *Partial Differential Equations*. Providence, RI: Amer. Math. Soc., 1998.
- [31] H. Zhao, T. Chan, B. Merriman, and S. Osher, "A variational level set approach to multiphase motion," *J. Comput. Phys.*, vol. 127, no. 1, pp. 179–195, Aug. 1996.
- [32] D. Adalsteinsson and J. Sethian, "A fast level set method for propagating interfaces," *J. Comput. Phys.*, vol. 118, no. 2, pp. 269–277, May 1995.
- [33] D. Adalsteinsson and J. Sethian, "The fast construction of extension velocities in level set methods," *J. Comput. Phys.*, vol. 148, no. 1, pp. 2–22, Jan. 1999.
- [34] C. Li, C. Xu, K. Konwar, and M. D. Fox, "Fast distance preserving level set evolution for medical image segmentation," in *Proc. 9th Int. Conf. Control Autom. Robot. Vis.*, 2006, pp. 1–7.
- [35] G. Gilboa, N. Sochen, and Y. Zeevi, "Forward-and-backward diffusion processes for adaptive image enhancement and denoising," *IEEE Trans. Image Process.*, vol. 11, no. 7, pp. 689–703, Jul. 2002.